ISSN 1810-2328, Journal of Engineering Thermophysics, 2024, Vol. 33, No. 1, pp. 200–219. © Pleiades Publishing, Ltd., 2024.

Fundamentals of Hydrodynamics and Heat and Mass Transfer at Film Condensation of Stationary Vapor on Horizontal Tube Bundles: A Brief Review

I. I. Gogonin[1] and O. A. Volodin[1*]

[1] *Kutateladze Institute of Thermophysics, Siberian Branch, Russian Academy of Sciences, Novosibirsk, Russia*

Received October 24, 2023; in final form, January 29, 2024; accepted February 2, 2024

Abstract—Condensers represent an indispensable part of equipment of any power, chemical-technological, cryogenic, refrigeration and other installations used in industry. Reducing the weight, dimensions and cost of devices is always an urgent task. The process of condensation in real devices is a very complex phenomenon. The intensity of energy transfer from vapor to a solid cooled wall is determined, other things being equal, by three interrelated factors: (i) variable irrigation density and change in film flow hydrodynamics as the irrigation density changes, (ii) variable vapor velocity affecting a condensate film in the varying film and vapor flow regimes, and (iii) effect of the diffusion process on heat transfer during condensation of vapor with non-condensable impurities. The authors consider that they have to describe the issues that are poorly covered in the literature, although these issues are of fundamental importance for understanding the process under study. In this paper, the main factors that determine heat transfer during stationary vapor condensation on horizontal tube bundles are considered. An algorithm for calculating a condenser at film condensation of stationary vapor without non-condensable impurities is proposed. A critical analysis of modern experimental studies on heat transfer during condensation has been carried out.

DOI: 10.1134/S1810232824010144

INTRODUCTION

Studies on heat transfer during vapor condensation have been carried out since the century before last; for example, the first research of this kind on vapor condensation on the outer wall of a tube with a wire wound in a spiral by Joule (1861) is well known [1]. Publications in various journals [2–12], periodic reviews [13–16] and theses [17, 18] reflect the state of research and progress in this field. Monographs on heat transfer [19–26] and reference books (such as "HEI Standards for Steam Surface Condensers" [27]), which deal with various issues of hydrodynamics and heat and mass transfer during vapor condensation outside and inside the bundles of horizontal and vertical smooth and profiled tubes, continue to be published.

The process of film condensation considered in this work, as a rule, occurs on hydrophilic surfaces, in contrast to drop condensation, which occurs on hydrophobic surfaces and coatings. Drop condensation is more efficient in terms of heat transfer, however, at present, most of industrial condensers that use ordinary metal tubes (without surface treatment or promoters) work using film condensation, since it has not yet been possible to achieve stable drop condensation for a long time.

Since publishing the seminal work by Nusselt (1916) [28], the understanding of the film condensation process has advanced considerably. However, even in studies on film condensation of stationary vapor, there are still some critical nuances, such as the presence of non-condensable impurities, which, even in very small fractions, can significantly reduce the values of experimental data on heat transfer. These nuances are not taken into account by the authors of some works, and this can lead to obtaining the results with a systematic error.

[*] Corresponding author. E-mail: volodin_o@mail.ru

The current review covers the issues of film condensation of stationary vapor on horizontal tube bundles in detail (using an extensive array of experimental data obtained by I.I. Gogonin and colleagues), including those that, despite the abundance of existing studies, are poorly presented in the literature. The review is limited to consideration of the issues of stationary vapor condensation only because of limitations on the paper format. The authors plan to consider the issues of condensation of moving vapor, as well as condensation of vapor on tube bundles with modified surfaces in future papers.

1. THE FEATURES OF HYDRODYNAMICS OF FLOWING FILM UNDER THE FORCE OF GRAVITY

In the fundamental work of Brauer [29], it was found that when a film flows down a vertical wall, three distinct regimes are observed: laminar, wave, and turbulent. In addition, the transitional regimes can be noted—laminar-wave and undeveloped turbulence regime.

The established fact of the conservatism of residual film thickness δ_0 with respect to the total flow rate of liquid is of fundamental importance. This result was later confirmed in [30, 31]. However, the dependences obtained for the first time in [29] can be considered fundamental.

The results of these experiments are shown in Fig. 1. It is clearly seen that the residual film thickness is almost independent of the film Reynolds number Re and depends significantly on the physical properties of liquid (the Kapitza number Ka).

It should be noted that in these works the measurements of residual layer thickness during the water film flow differ quantitatively from each other. The dependence obtained for the first time in [29] can be considered only as a first approximation.

As it is shown in [31], the intrinsic wave regime on the residual layer does not have time to develop due to the short time of its existence, which is approximately equal to the wave period.

It can be assumed that the bulk of liquid, determined from the total irrigation density, is transported in waves, and the main thermal resistance of the film is determined by the residual layer, whose thickness remains almost constant over a wide range of changes in the film Re number.

Perturbations (waves) of relatively large amplitude propagate with a certain velocity over the residual layer δ_0, and an increase in the flow rate of liquid leads not to an increase in δ_0, but to a decrease in wavelength λ. An analysis of experimental data [31] on determination of the velocity profiles in wave film flows allows a conclusion that the velocity profile is semiparabolic, as in the case of a laminar flow. The heat transfer coefficient can be estimated from the residual film thickness δ_0 and its heat conductivity:

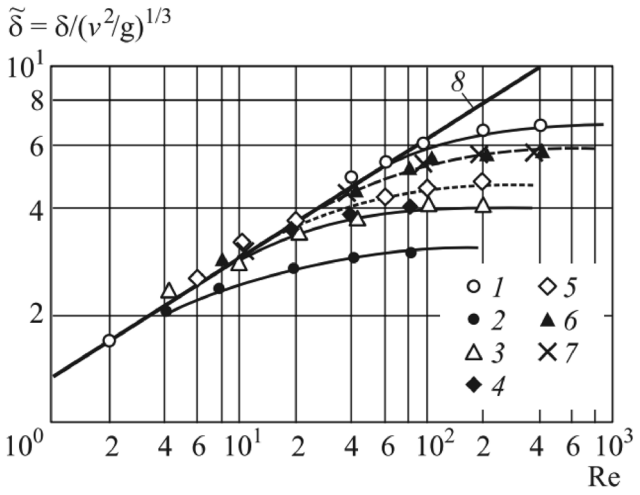

Fig. 1. Dependence of dimensionless film thickness on the Re number according to [29] (at $t_L = 20°$C): *1*—Ka $= 5.67 \cdot 10^{10}$; *2*—Ka $= 2.92 \cdot 10^5$; *3*—Ka $= 4 \cdot 10^6$; *4*—Ka $= 5.6 \cdot 10^7$; *5*—Ka $= 3.6 \cdot 10^8$; *6*—Ka $= 2.2 \cdot 10^9$; *7*—Ka $= 8.8 \cdot 10^9$; *8*—calculation by the Nusselt theory.

$$\alpha_w = \lambda/\delta_0. \tag{1}$$

The character of dependence of the average residual layer thickness $\overline{\delta_0}$ (experimental points 1–7) and the average Nusselt film thickness $\overline{\delta}$ on the Reynolds number can be judged from the data of [29] shown in Fig. 1. It can be seen from the figure (in which the values are presented in dimensionless form) that, up to a certain value of Re_*, the residual and average film thicknesses coincide and can be determined from the dependence:

$$\overline{\delta} = \overline{\delta_0} = 3\mathrm{Re}^{-1/3}. \tag{2}$$

In [29], the dependence of Re_* on liquid properties was experimentally established, and it can be represented as:

$$\mathrm{Re}_* = 2.3\mathrm{Ka}^{1/10}. \tag{3}$$

The numerical value of $\overline{\delta_0}$ at $\mathrm{Re} = \mathrm{Re}_*$ is determined by substituting (3) into (2):

$$\overline{\delta_{0*}} = 1.9\mathrm{Ka}^{1/30}. \tag{4}$$

Since residual layer thickness $\overline{\delta_0}$, determined by (4), is independent of the Re number within $\mathrm{Re}_* < \mathrm{Re} < \mathrm{Re}_{cr}$, the average heat transfer coefficient in the wave region can be immediately determined from (1) and (4):

$$\alpha_w \cdot l_\nu/\lambda = 0.527\mathrm{Ka}^{-1/30}. \tag{5}$$

The critical Reynolds number of the film, corresponding to the transition of a wave flow into a turbulent one [29], can be expressed by the dependence:

$$\mathrm{Re}_{cr} = 35\mathrm{Ka}^{1/10}. \tag{6}$$

The following should be noted for the turbulent film flow. In the case of heat transfer without a phase transition, when the heat flux changes from zero on the film surface to a maximum value on the wall, the transfer in a viscous sublayer is decisive. During condensation, the heat flux distribution over the film cross-section is almost uniform, and therefore the mechanisms of turbulent transfer over the entire film cross-section are essential.

To achieve a more detailed description of the turbulent transfer mechanism, the work [32] considers a model, in which the turbulent viscosity is piecewise approximated by dependences:

$$0 < \hbar < 6.8, \quad \widetilde{\mu_t} = 0,$$

$$6.8 < \hbar < 0.2\,(\hbar_\delta - 6.8)\,; \quad \widetilde{\mu_t} = 0.4\,(\hbar - 6.8)\sqrt{1 - \frac{\hbar}{\hbar_\delta}}, \tag{7}$$

$$0.2\,(\hbar_\delta - 6.8) < \hbar < \hbar_\delta; \quad \widetilde{\mu_t} = 0.08\,(\hbar - 6.8)\sqrt{1 - \frac{\hbar}{\hbar_\delta}}.$$

In this model, the length of the mixing path beyond the viscous sublayer is counted from its conditional boundary $\hbar = 6.8$, which correlates with the value of the Prandtl–Karman constant $\chi = 0.4$.

The dimensionless film thickness is related to the Reynolds number by the following relationship, obtained under the assumption of a linear distribution of friction over the film cross-section:

Table 1. The average values of Nusselt number $\overline{\mathrm{Nu}_t^*}$, obtained by numerical calculation [32]

Pr	$\hbar_\delta$ Re	60 742	100 1516	200 3697	300 6047	1000 24244	4000 112432
1	—	0.157	0.160	0.168	0.176	0.213	0.285
2	—	0.212	0.223	0.245	0.262	0.332	0.452
3	—	0.252	0.270	0.300	0.324	0.416	0.572
5	—	0.307	0.332	0.377	0.410	0.532	0.735
7	—	0.344	0.374	0.428	0.467	0.607	0.841
10	—	0.382	0.418	0.479	0.523	0.682	0.948

$$\mathrm{Re} = \int_0^{\hbar_\delta} \varphi(\hbar)d\hbar = \overline{\varphi}\hbar_\delta. \tag{8}$$

The values of the Nusselt number during the turbulent film flow are calculated by relationships:

$$\mathrm{Nu}_t^* = \hbar_\delta^{1/3}\left(\int_0^{\hbar_\delta} \frac{d\hbar}{1+\mathrm{Pr}\,\widetilde{\mu}_t}\right)^{-1}, \tag{9}$$

where $\hbar = \frac{v^* y}{\nu}$ is dimensionless distance from the wall; $\widetilde{\mu}_t = \mu_t/\mu$; $\hbar_\delta = \frac{v^*\delta}{\nu}$ is dimensionless film thickness. Here $v^* = \sqrt{\frac{\tau_W}{\rho_L}}$ is shear velocity [m/s].

The results of numerical calculation of average Nusselt number $\overline{\mathrm{Nu}_t^*}$ for some integer values of the Prandtl number are presented in Table 1, see [32] for details.

2. CONDENSATION OF STATIONARY VAPOR ON A SINGLE HORIZONTAL CYLINDER OF A VARYING DIAMETER

The Nusselt solution [28] on heat transfer during vapor condensation on a single horizontal cylinder was presented by Colburn [33] in dimensionless coordinates in the form:

$$\mathrm{Nu}^* = 0.754\mathrm{Re}^{-1/3}, \tag{10}$$

Here $\mathrm{Re} = \frac{\pi Dq}{2\mu r} = \frac{G}{2\mu}$ is Reynolds number for the film; where $G = \frac{\pi Dq}{2r}\left[\frac{\mathrm{kg}}{\mathrm{m\cdot s}}\right]$ is the density of irrigation of the half-perimeter of the tube; $\mathrm{Nu}^* = \alpha\lambda/\left(\frac{\nu^2}{g}\right)^{1/3}$ is the Nusselt number for the film.

The largest number of experimental works published to date has been carried out with the condensation of steam under reduced pressure. The reliability of these data is quite low [34, 35]. In [34], Berman compared the experimental data on steam condensation on a single horizontal cylinder with the calculation by the Nusselt theory in coordinates $\alpha/\alpha_0 = f(\Delta t)$. Here, α and α_0 are the experimental and calculated values of the heat transfer coefficient; $\Delta t = t_S - t_W$ is the temperature difference between steam and wall. It is shown that at low temperature differences the scatter of experimental data reaches ±75%; and at high Δt, it decreases to ±25%.

The results of processing the data of some other researchers [36–44] are presented in Fig. 2 in coordinates $\mathrm{Nu}^* = f(\mathrm{Re})$.

The analysis was carried out for condensation of stationary steam on a smooth single horizontal cylinder. There is a significant scatter of data, which is not accidental and is explained by two fundamentally different reasons:

(a) When conducting subatmospheric pressure experiments, there is a very high probability that an uncontrolled amount of air will enter the installation. Ultimately, this leads to a decrease in the heat transfer coefficient.

(b) As it can be seen from the captions to Fig. 2, most experiments were carried out on tubes with dimensionless diameter $\widetilde{D} < 10$. As it will be shown below, under these conditions the influence of cylinder diameter, leading to heat transfer intensification during condensation, begins.

Below are the measurement results on heat transfer during condensation of various refrigerants.

If the condensation process occurs on cylinders which diameters are comparable with the capillary constant, then the film hydrodynamics will be largely determined by the forces of surface tension. In this case, heat transfer during condensation depends on the ratio of the cylinder diameter to the capillary constant or on dimensionless parameter $\widetilde{D} = D/\sqrt{\frac{\sigma}{g(\rho_L - \rho_V)}}$.

The experimental results on freon R12 condensation on horizontal cylinders of different diameters are shown in Fig. 3. Data for cylinders with $D = 10$, 16, and 45 mm are described by one dependence.

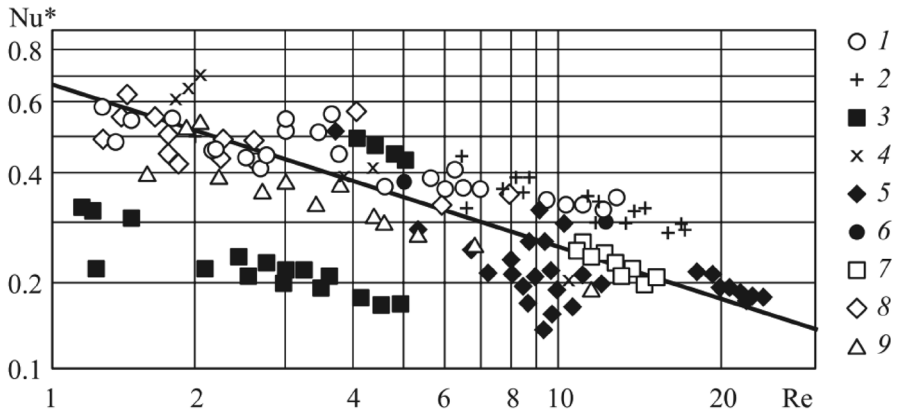

Fig. 2. Heat transfer at steam condensation on the horizontal cylinder [35]: *1*—[36], $\widetilde{D} = 6.45$; *2*—[37], $\widetilde{D} = 4.5$–6.4; *3*—[38], $\widetilde{D} = 7.05$–7.25; *4*—[39], $\widetilde{D} = 7.4$; *5*—[40], $\widetilde{D} = 4.8$; *6*—[41], $\widetilde{D} = 7.2$–7.6; *7*—[42], $\widetilde{D} = 5.1$; *8*—[43], $\widetilde{D} = 7.2$; *9*—[44], $\widetilde{D} = 7.2$–7.4. Line—calculation by the Nusselt theory.

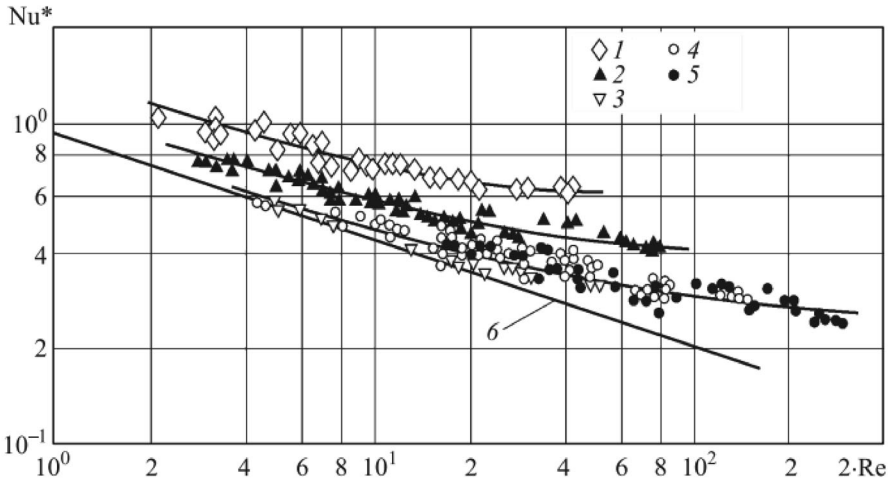

Fig. 3. Heat transfer at condensation of refrigerant R12 on a single horizontal cylinder [45]: *1*—$D = 3$ mm; *2*—$D = 6$ mm; *3*—$D = 10$ mm; *4*—$D = 16$ mm; *5*—$D = 45$ mm; *6*—calculation by the Nusselt theory [28].

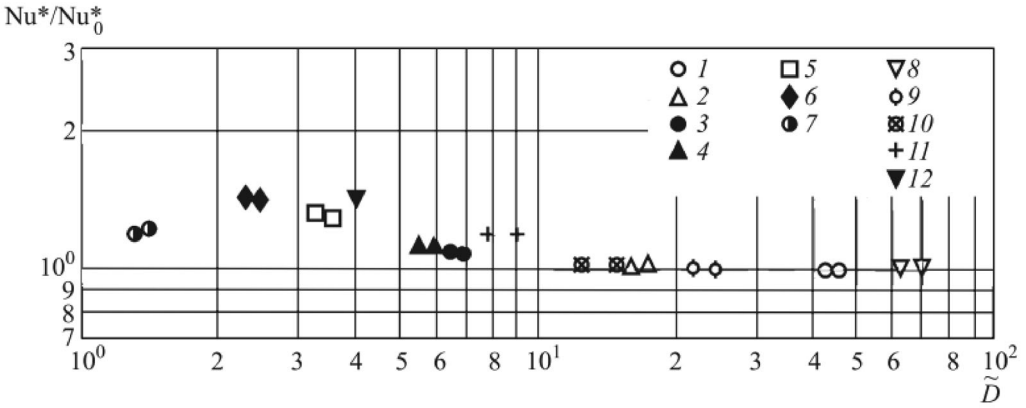

Fig. 4. Relative change in the Nusselt number vs. dimensionless diameter [45], Re = 5. R21, $t_S = 30$–$90^\circ C$: *1*—$D = 45$ mm; *2*—$D = 17$ mm; *3*—$D = 7$ mm; *4*—$D = 6$ mm; *5*—$D = 3.6$ mm; *6*—$D = 2.5$ mm; *7*—$D = 1.5$ mm. R12, $t_S = 40$–$85^\circ C$: *8*—$D = 45$ mm; *9*—$D = 16$ mm; *10*—$D = 10$ mm; *11*—$D = 6$ mm; 12—$D = 3$ mm.

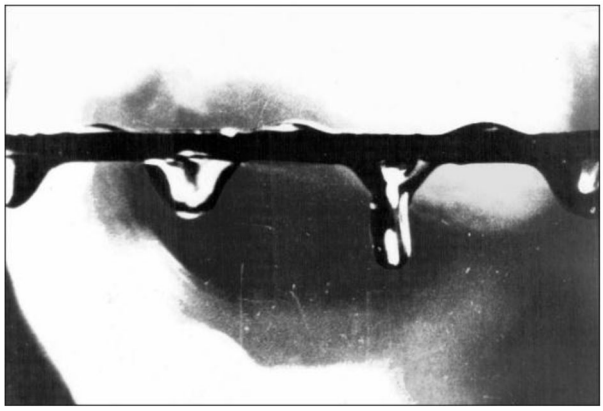

Fig. 5. Vapor condensation on a cylinder with a diameter comparable to the capillary constant [45], refrigerant R21, $t_S = 50^\circ C$, $D = 1.2$ mm, Re = 4.

The intensity of condensation on cylinders of small diameter $D = 6$ and 3 mm increases significantly. The processing of experimental results in coordinates $\mathrm{Nu}^*/\mathrm{Nu}_0^* = f(\widetilde{D})$ at Re = const demonstrates the ambiguous effect of the cylinder diameter on heat transfer (Fig. 4). In the laminar regime, it is necessary to distinguish two characteristic regions. At $\widetilde{D} < 10$, heat transfer depends on two parameters: the Re number and dimensionless diameter $\widetilde{D}$. At $\widetilde{D} > 10$, on cylinders of a large diameter, heat transfer is characterized only by the film Reynolds number Re. In the general case, heat transfer during film condensation on a single horizontal cylinder depends on the film Reynolds number, the dimensionless diameter, and the film Kapitza number Ka.

A frame of the high-speed video of vapor condensation on a cylinder with a diameter comparable with the capillary constant is shown in Fig. 5. It is clearly seen that even at low Re numbers, a wave character of film motion is observed. After droplet separation, the surface tension forces pull liquid to the cylinder, it overcomes short distance $\pi \cdot R$ by inertia and reaches the top point of the cooled tube. This means that during condensation on cylinders of small diameter $\widetilde{D} < 10$, there is no laminar film flow at all, and the resulting capillary waves intensify heat transfer during condensation.

3. HYDRODYNAMICS AND HEAT TRANSFER AT VAPOR CONDENSATION ON HORIZONTAL BUNDLES OF SMOOTH TUBES

A fundamentally important result on vapor condensation on a tube bundle is presented in [45, 46]. The experiments on condensation of R21 were conducted on a ten-row bundle of tubes. On each

tube, the specific heat flux and the average wall temperature were the determined parameters. The measurement results in coordinates $\alpha = f(\Delta t)$ are presented in Fig. 6. For the first (upper) tube, the measured experimental results are close to those calculated using the Nusselt formula [28]. As the tube number increases, the heat transfer intensity decreases, and dependences $\alpha = f(\Delta t)$ change qualitatively. It can be seen that for the lower tubes of the bundle, the heat transfer coefficient in the studied range of parameters does not depend on the temperature difference or on the number of the tube in the bundle.

In dimensionless coordinates (Fig. 7) these experimental results were processed in [45] in the form $\mathrm{Nu}^* = f(\mathrm{Re})$, were

$$\mathrm{Re} = \pi R \sum_{1}^{n} q_i/\mu r. \tag{11}$$

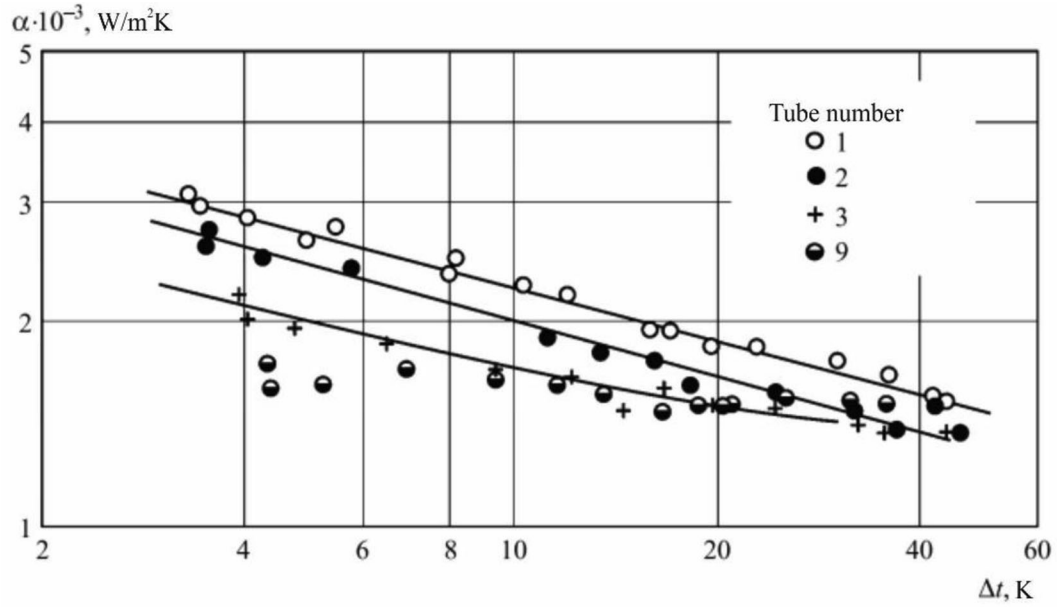

Fig. 6. Dependence of the heat transfer coefficient on the temperature difference at condensation of stationary vapor on a bundle of horizontal tubes [46]: refrigerant R21, $D = 16$ mm, $S/D = 1.87$ (where S is pitch of tubes in bundle).

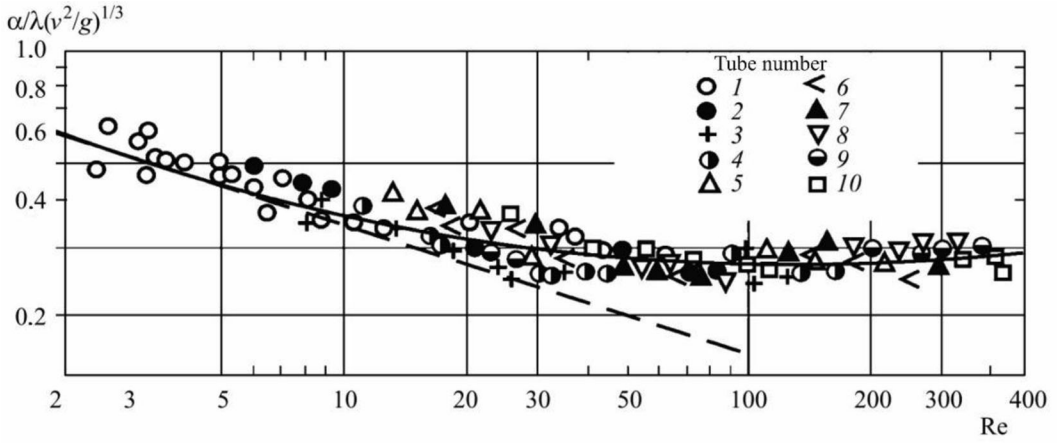

Fig. 7. Heat transfer at condensation of stationary vapor on a bundle of horizontal tubes [46]: refrigerant R21, $t_S = 40$; 90°C; $D = 16$ mm; dashed line—calculation by the Nusselt theory.

In these works, it was shown for the first time that the determining parameter of heat transfer during vapor condensation on a tube bundle is the total irrigation density G [kg/(m·s)] or in dimensionless form—the Re number, derived from the total irrigation rate of cylinder.

The results on condensation of refrigerant R12 on a tube bundle, where the laminar, wave and turbulent film flows were achieved in one experiment, are presented in Fig. 8. This figure also shows

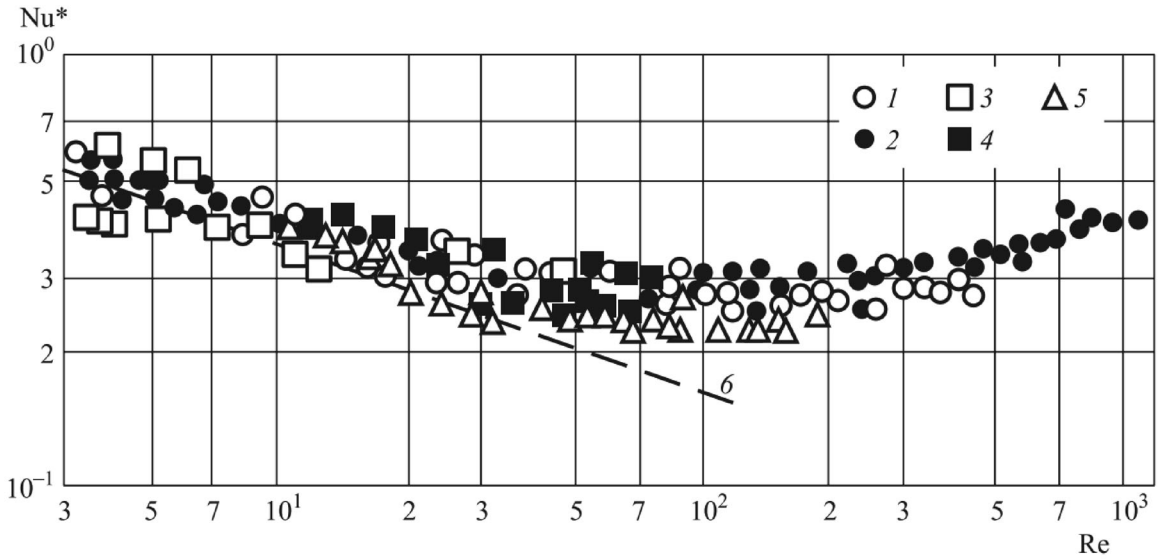

Fig. 8. Heat transfer at condensation of various vapors on tube bundles: *1*—R21: Re = 2–420 [46, 47]; *2*—R12: Re = 3–1100 [47]; *3*—R12: Re = 7.5–96 [48]; *4*—R11: Re = 4–55 [49]; *5*—R134a: Re = 10–190 [51]; *6*—calculation by formula (10).

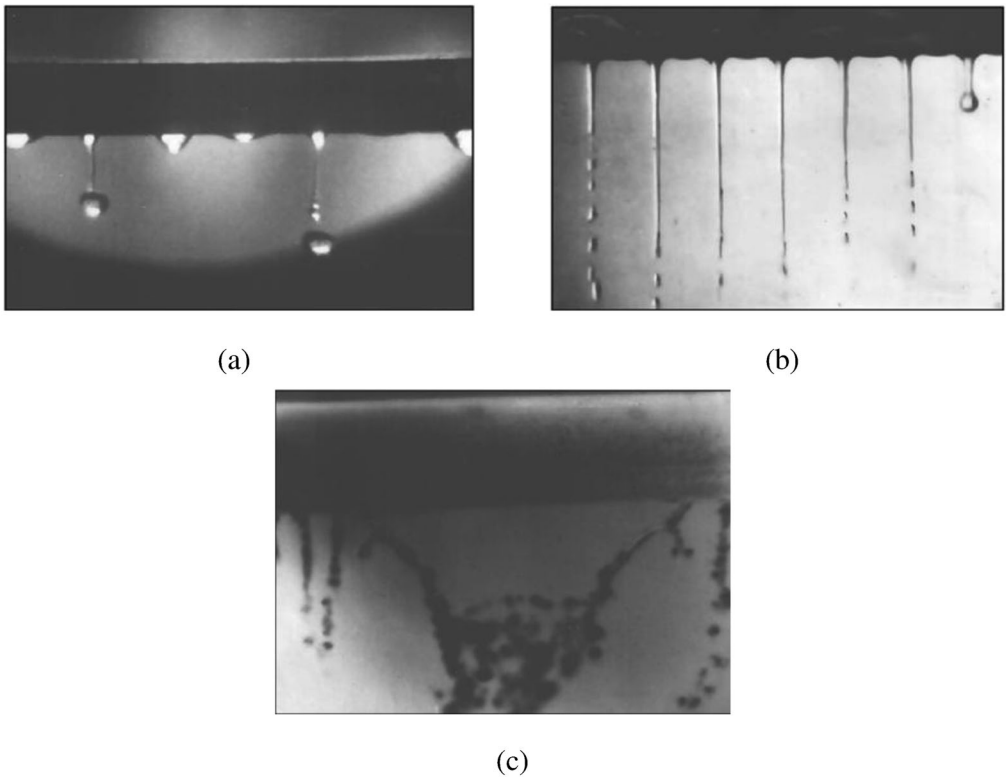

Fig. 9. Typical regimes of condensate flow from a horizontal cylinder (R12): (a) $t_S = 40°C$, Re = 12; (b) $t_S = 60°C$, Re = 40; (c) $t_S = 85°C$, Re = 65 [45].

a satisfactory agreement between the data of different authors obtained at condensation of various refrigerants, which confirms the decisive role of the heat transfer dependence on the irrigation rate of a given tube in the bundle.

When processing experiments performed at $t_S = 80$–$90°C$ and with a turbulent film flow, a correction factor, equal to the ratio of the Prandtl number Pr at the experiment temperature to the value of Pr at $t_S = 60°C$ was introduced: $(\mathrm{Pr}/\mathrm{Pr}_0)^{0.4}$. Satisfactory coincidence of data from different authors given in Fig. 8 relates to the fact that the experiments were carried out at condensation of vapors of liquids with similar physical properties and with almost the same geometric parameters of tube bundles.

The typical regimes of condensate (R12) flow from a cooled cylinder are presented in Fig. 9. At low Re numbers, the droplet regime is observed (Fig. 9a), and as the Re number increases, it turns into the jet regime (Fig. 9b). A photograph of the liquid flow in the form of a continuous film is presented in Fig. 9c. Such a flow occurs only under the near-critical pressure at sufficiently high irrigation densities, i.e. under the condition that the surface tension of liquid tends to zero.

In some papers cited in reviews [14–16], it is proposed to represent generalization of experimental results on heat transfer during vapor condensation on tube bundles in the form:

$$\alpha_n/\alpha_i = f(n). \tag{12}$$

However, empirical formulas in the form of polynomial equations, which include the number of the tube in the bundle, are not capable of describing the entire array of experimental data. In most cases, dependence (12) cannot be considered correct. As a rule, the laminar film flow occurs on the first tube of the bundle, and on the nth tube, the film flow is most often turbulent or wavy. Comparison of data of dependence (12) obtained for different film flows cannot be considered correct.

The experimental data processing in the form of dependence $\mathrm{Nu}^* = f(\mathrm{Re})$ allows consideration of the effect of irrigation density on heat transfer. The dependence presented in Figs. 7 and 8 distinguishes clearly all film flows depending on the Re number.

Another fundamentally important result is the measurement of liquid temperature in-between the tubes [51]. The experiments have shown that each underlying tube receives condensate at the saturation temperature. Figure 10 shows how the temperature of condensate changes in space between the tubes. The supercooled liquid after separation heats up very quickly and reaches the

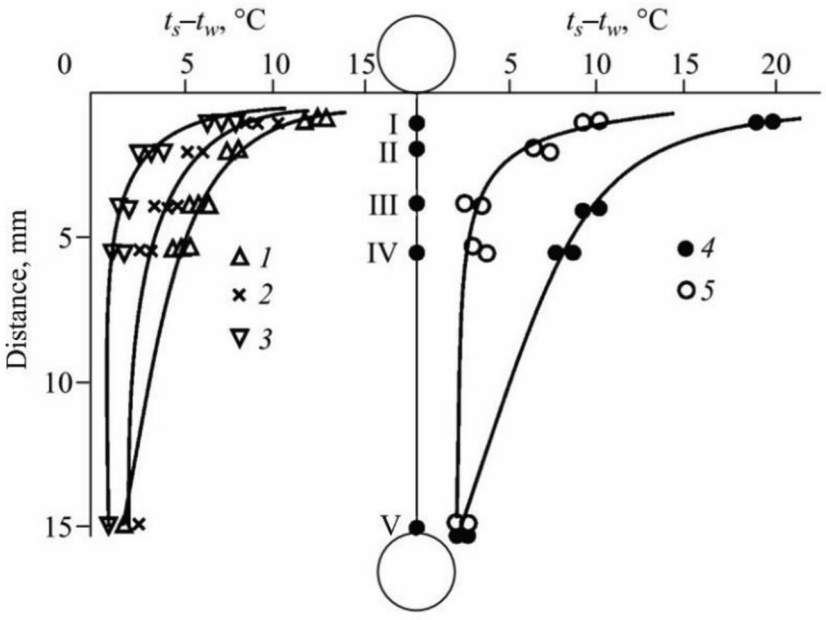

Fig. 10. Layout of thermocouples and diagrams of condensate (R12) temperatures in space between the tubes $t_S = 60°C$, $\Delta t = 35°C$: *1*—Re = 35, *2*—Re = 150, *3*—Re = 250; $t_S = 70°C$, $\Delta t = 50°C$: *4*—Re = 60, *5*—Re = 250; I–V—points of thermocouple location [51].

saturation temperature. Intensive condensation occurs on supercooled drops and jets. The rate of condensate warmup increases with an increase in the irrigation density.

The warmup of the condensate, flowing onto the underlying tube in the bundle, to $t_L = t_S$ stops condensation on the upper part of the lateral surface of this tube. In this section with length L_{ENT}, heat will be transferred only by convection from a heated film with temperature t_S to a cold wall. Condensation will begin at some distance from the point where the liquid falls onto the tube. In other words, an entrance region of the thermal boundary layer appears in the film. In this case, the following situations are possible:

(a) the length of the entrance region is greater than the half-perimeter of the tube. Due to convection, the liquid is supercooled, and condensation occurs completely in-between the tubes on drops and jets;

(b) at $L_{ENT} \ll \pi R$ condensation on the tube bundle is almost the same as on a vertical surface;

(c) if the length of the entrance region L_{ENT} is less than tube half-perimeter $L = \pi R$, both convective heat transfer and condensation take place;

(d) with a dense arrangement of tubes in the bundle, a condensate drop flows smoothly onto the tube located below and does not have time to change the temperature noticeably. Such a bundle of tubes should be considered as a vertical wall.

Experimental studies in a wide range of changes in the parameters of condensation on a bundle of horizontal tubes have shown the decisive influence of irrigation density and film flow hydrodynamics on heat transfer.

A simplified diagram of the liquid flow in the tube bundle is shown in Fig. 11. A liquid film with temperature t_L (in the general case, $t_L < t_S$), initial thickness δ_0 and velocity u_0 flows down a cylindrical wall of length $L = \pi R$ and temperature t_W.

The value of angle φ, when the thermal boundary layer reaches the film thickness, can be calculated from the relationship derived in [51]:

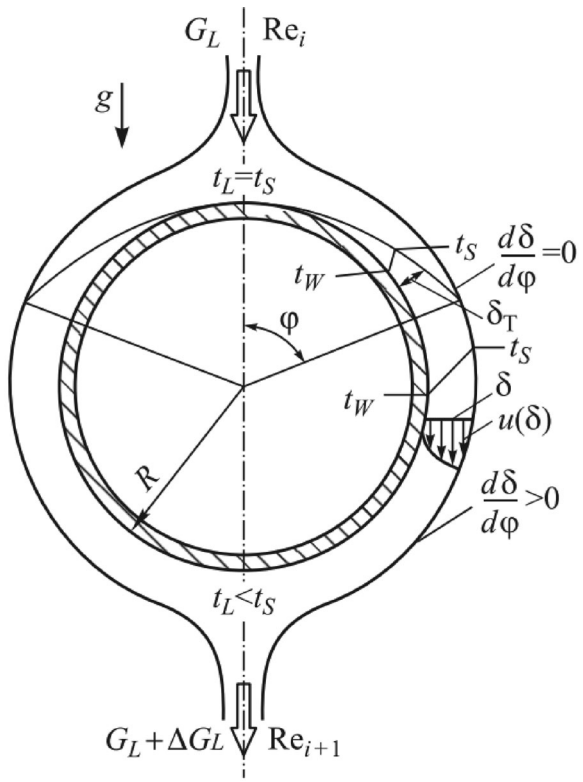

Fig. 11. Scheme of liquid flow in a bundle of horizontal tubes.

Table 2. Values of $P(\varphi)$, $Q(\varphi)$, and $Q(\varphi)/\varphi$

φ, deg	$P(\varphi)$	$Q(\varphi)$	$Q(\varphi)/\varphi$	φ, deg	$P(\varphi)$	$Q(\varphi)$	$Q(\varphi)/\varphi$
0	0	0	—	100	1.469	1.939	1.111
10	0.073	0.260	1.49	110	1.641	2.088	1.088
20	0.184	0.489	1.401	120	1.810	2.229	1.064
30	0.315	0.697	1.331	130	1.974	2.361	1.040
40	0.779	0.896	1.283	140	2.129	2.483	1.016
50	0.615	1.088	1.247	150	2.273	2.594	0.991
60	0.779	1.272	1.215	160	2.404	2.696	0.965
70	0.948	1.449	1.186	170	2.515	2.777	0.936
80	1.120	1.619	1.160	180	2.589	2.824	0.899
90	1.295	1.783	1.135				

$$P(\varphi) = \int_0^{\varphi} (\sin\varphi)^{1/3}\, d\varphi = 0.605 \mathrm{PrRe}^{4/3}\mathrm{Ga}^{-1/3} \tag{13}$$

and Table 2, which presents the values of function $P(\varphi)$.

The dependence for Nusselt number determining in the entrance region, derived in [51], is reduced to the form:

$$\mathrm{Nu}^*_{ENT} = 1.13\mathrm{Pr}^{1/3}\mathrm{Re}^{1/9}\mathrm{Ga}^{-1/9}Q(\varphi)/\varphi. \tag{14}$$

The values of $Q(\varphi) = \int_0^{\varphi} (\sin\varphi)\,/P(\varphi)^{1/3}\, d\varphi$ are given in Table 2.

Their weak dependence on the Reynolds number and the influence of the linear size on the final result through the Ga criterion follow from expression (13) for heat transfer in the entrance region. Two series of experiments can serve as experimental confirmation of this fact. In the first one, the diameters of tubes in the bundle were changed, and in another, the free fall velocity of condensate flowing onto the experimental tube was changed.

Data on heat transfer in bundles of tubes with diameters from 3 to 45 mm, processed in coordinates $\mathrm{Nu}^* = f(\mathrm{Re})$, are shown in Fig. 12. The results for bundles of tubes with $D = 10$, 16, and 45 mm almost coincided with each other. Heat transfer on small tubes ($D = 3$ and 6 mm) is noticeably higher, and the data begin to depend on the tube diameter. Such an increase in the heat transfer intensity is associated with waves at the interface and with a relatively large contribution of the entrance region section with convective heat transfer. A common feature of all experiments is the presence of a quasi-self-similarity region in heat transfer when the Reynolds number varies over a wide range.

A decrease in the diameter of tubes in the bundle decreases the lower boundary of the wave influence region to $\mathrm{Re} \approx 10$, while on the tubes of a large diameter it corresponds to $\mathrm{Re} \approx 40$. Visual observations and high-speed filming showed that at high irrigation densities, the jet separation points move periodically along the tube perimeter, and jets oscillate.

In Fig. 13, the results of these measurements are presented in coordinates $\mathrm{Nu}^*/\mathrm{Nu}^*_0 = f(\widetilde{D})$ for two essentially different Reynolds numbers of the film. It was found that during condensation on a bundle, the influence of the cylinder diameter is noticeably stronger ($\mathrm{Re} = 150$) than during condensation on single tubes ($\mathrm{Re} = 5$). In relation ($\mathrm{Nu}^*/\mathrm{Nu}^*_0$), the value of Nu^*_0 corresponds to a region, self-similar with respect to the heat transfer diameter ($\widetilde{D} > 20$).

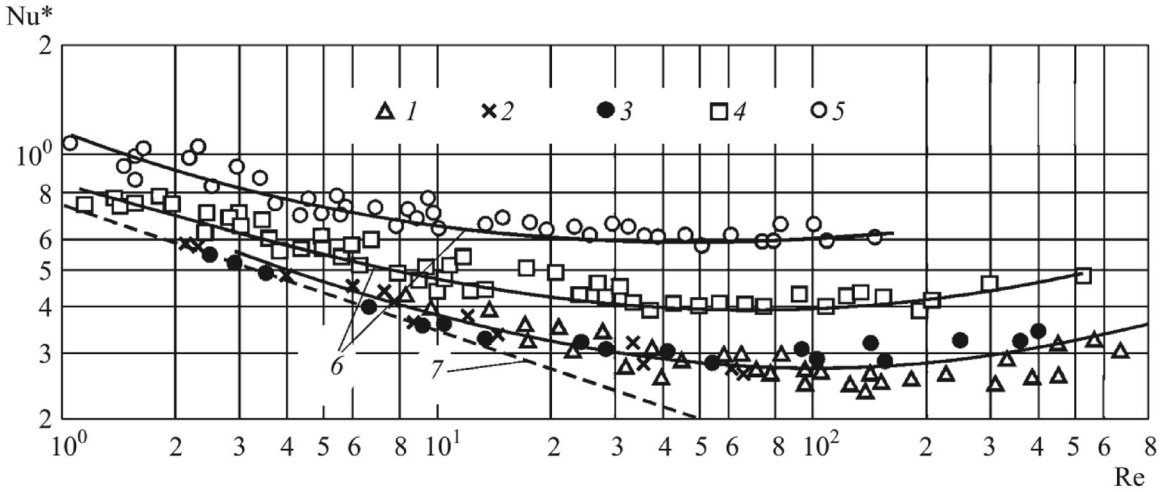

Fig. 12. Heat transfer during condensation on the bundle of tubes of different diameters [51], R12: *1*—$D = 45$ mm; *2*—$D = 16$ mm; *3*—$D = 10$ mm; *4*—$D = 6$ mm; *5*—$D = 3$ mm; *6*—lines, which average the experimental results; *7*—calculation by the Nusselt theory.

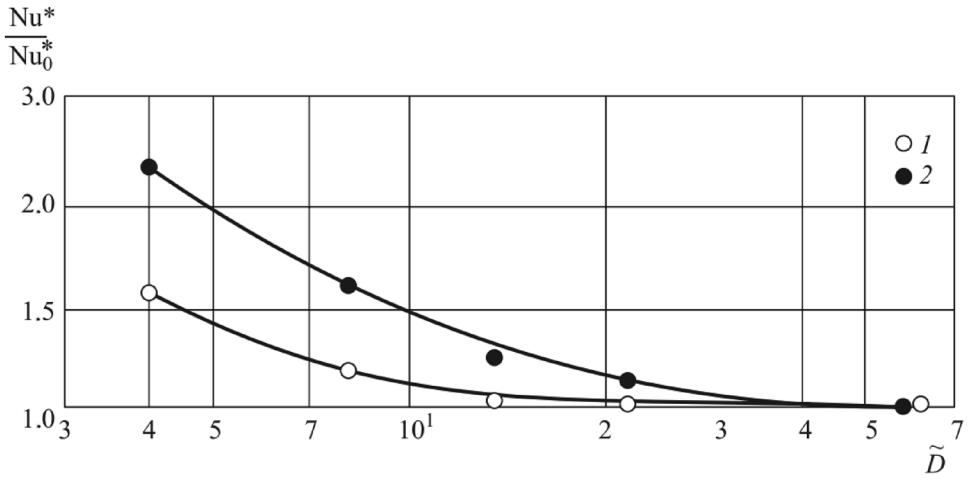

Fig. 13. A relative change in heat transfer during condensation on single tubes and tube bundles: *1*—Re = 5; *2*—Re = 150 [51].

It was shown above that intensification of heat transfer on single cylinders of a small diameter is associated with the influence of surface tension forces. Additional intensification on the bundles of such tubes is associated with low thermal resistance to convective heat transfer in the entrance region of the thermal boundary layer.

The effect of the free fall velocity of condensate on the heat transfer intensity is shown in Fig. 14. Its change by a factor of 2 does not lead to a significant change in heat transfer in a wide range of the film Reynolds numbers. The experimental values of Nu_1^* and Nu_2^* were obtained during condensation on the bundles with different distances between the tubes.

It was noted above that the length of the entrance region can either exceed the tube half-perimeter or be a part of it. If L_{ENT} exceeds the tube half-perimeter, then only convective heat transfer occurs there, which is determined from dependence (15) at $\varphi = \pi$:

$$\mathrm{Nu}_{ENT}^* = 1.01\mathrm{Pr}^{1/3}\mathrm{Re}^{1/9}\mathrm{Ga}^{-1/9}. \tag{15}$$

The results in Fig. 15 show the correspondence between the experimental and calculated values of heat transfer for the bundles of tubes with a small diameter. The result obtained confirms condensation in-between the tubes and convective heat transfer on them.

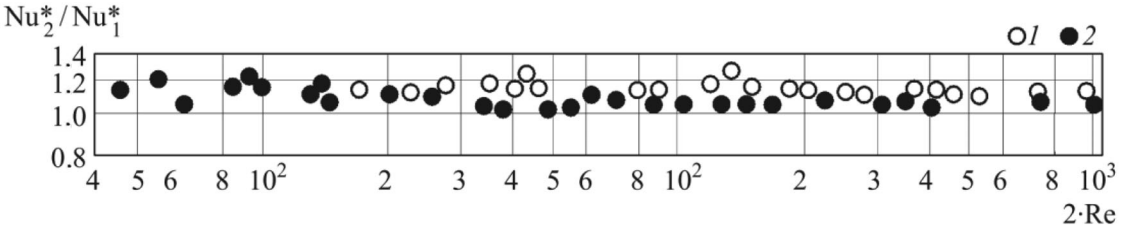

Fig. 14. The effect of condensate fall velocity on heat transfer [53] (R12): *1*—$D = 16$ mm, Nu_1^* at $U_1 = 0.54$ m/s; Nu_2^* at $U_2 = 1.23$ m/s; *2*—$D = 6$ mm Nu_1^* at $U_1 = 0.35$ m/s; Nu_2^* at $U_2 = 0.7$ m/s.

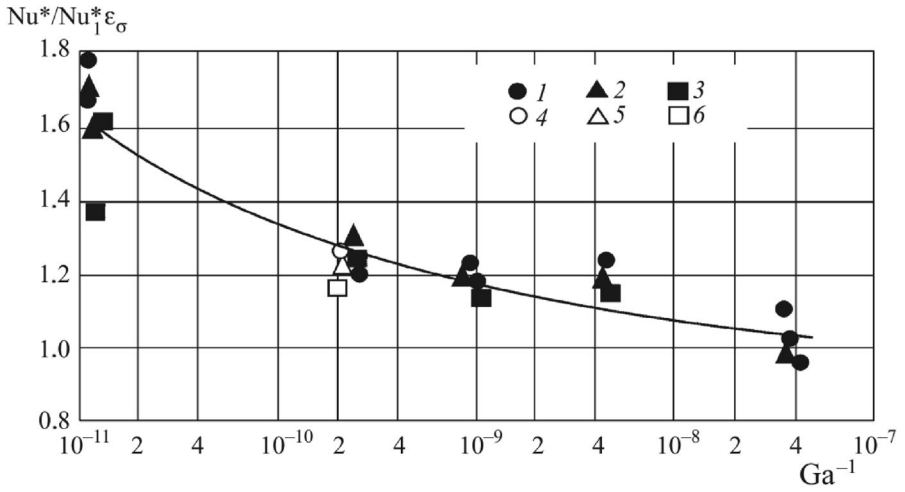

Fig. 15. Comparison of experimental values of Nu^* number with those calculated by (16) in dependence of the Galileo number [53]. R12: *1*—Re = 100; *2*—Re = 150; *3*—Re = 300. R21: *4*—Re = 100; *5*—Re = 150; *6*—Re = 300.

In the general case, heat transfer on the ith tube of the bundle is determined by dependence

$$\mathrm{Nu}^* = \frac{1}{\pi}\left[\left(\overline{\mathrm{Nu}_{ENT}^*}\right)\varphi + \left(\mathrm{Nu}_C^*\right)(\pi - \varphi)\right], \tag{16}$$

where $\overline{\mathrm{Nu}_{ENT}^*}$ is the average Nusselt number in the entrance region of the thermal boundary later; for the laminar and wave flows, it is calculated by dependence (13). Nu_C^* is the Nusselt number, which takes into account heat transfer on a part of tube surface where condensation occurs. The angle φ is measured in radians and is calculated from relation (13). When determining Nu_C^*, it was assumed that the film thermal resistance can be replaced by the resistance of the residual film thickness (5).

4. HYDRODYNAMICS AND HEAT TRANSFER DURING STEAM CONDENSATION ON BUNDLES OF SMOOTH HORIZONTAL TUBES

The experiments described in [36] were carried out carefully, aimed to obtain steam without non-condensable impurities. Before the experiments, distilled water was degassed in a steam generator. At that, an instantaneous release of pressure was periodically carried out and pool boiling of liquid was observed, i.e. it was completely degassed. The setup was filled with degassed water at excess pressure (up to $2.5 \cdot 10^5$ Pa). Before filling, the setup was vacuumed. The remaining air in each vessel of setup was displaced by degassed water until it was completely filled with liquid. The experiments were carried out at excess pressure on a cunial tube ($D = 16$ mm) installed at the bottom of a bundle of finned tubes. The saturation temperature was varied within 105–112°C. Excessive pressure in the setup was maintained twenty-four hours a day. This technique allowed

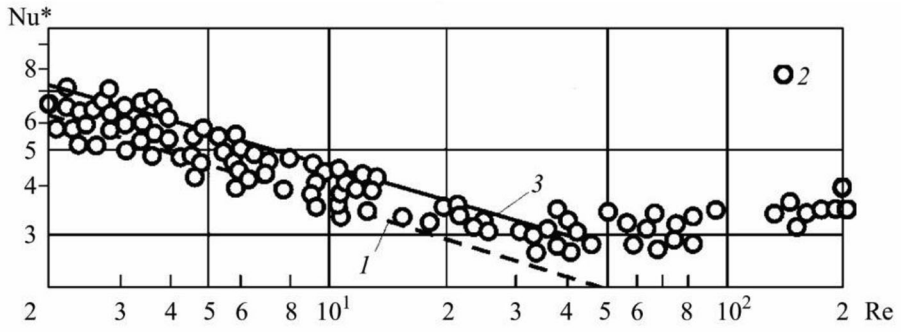

Fig. 16. Heat transfer during condensation of stationary steam on a bundle of horizontal tubes [36]: $t_S = 105°C$; $D = 16$ mm; *1*—calculation by the Nusselt theory; *2*—measurement results; *3*—calculation by formula (16).

obtaining steam without non-condensable impurities. The measurement results were repeated with numerous setup refilling. Each parameter was measured in two independent ways. The average temperature of the experimental tube was taken after averaging the readings of thermocouples mounted five at a time in two different cross-sections and placed along the perimeter in every 45°. The steam-wall temperature difference on the tube varied from 3 to 26°C, and the specific heat flux was up to $2.9 \cdot 10^5$ [W/m^2].

The measurement results are given in Fig. 16. In [36], the experimental results on heat transfer during steam condensation were compared with the results on condensation of refrigerants and, at the same $\widetilde{D}$ and Re, they coincided.

5. ALGORITHM FOR CALCULATING A CONDENSER DURING CONDENSATION OF STATIONARY VAPOR WITHOUT NON-CONDENSABLE IMPURITIES

The suggested calculation algorithm is based on two assumptions supported by experimental data:

(a) In the wave film flow, the main thermal resistance is the residual layer thickness, and the Nusselt number is calculated by formula (5).

(b) In the turbulent film flow, heat transfer is satisfactorily determined by the three-layer turbulence model (8), which was confirmed in [30–32].

Heat transfer on the ith tube of the bundle is determined by dependence (16) given above. The average Nusselt number during condensation and in the mixed film flow is determined from dependence:

$$\overline{\overline{\mathrm{Nu}^*}} = \overline{\mathrm{Nu}_l^*}\frac{\mathrm{Re}_*}{\mathrm{Re}} + \overline{\mathrm{Nu}_w^*}\frac{\mathrm{Re}_{cr} - \mathrm{Re}_*}{\mathrm{Re}} + \overline{\mathrm{Nu}_t^*}\frac{\mathrm{Re} - \mathrm{Re}_{cr}}{\mathrm{Re}}. \tag{17}$$

Here Re_* and Re_{cr} are calculated by (3) and (6). $\overline{\mathrm{Nu}_l^*}$ is the average Nusselt number at the laminar film flow, calculated by (10). $\overline{\mathrm{Nu}_w^*}$ is the average Nusselt number at the wave film flow on the bundle of tubes with $\widetilde{D} > 10$ calculated by dependence (16). $\overline{\mathrm{Nu}_t^*}$ is the average Nusselt number at the turbulent flow, see paragraph 1.

For the tubes with a smaller diameter, heat transfer in the entrance region of the thermal boundary layer should be taken into account for laminar and wave film flows. The experimental data obtained on bundles of tubes with $D = 16$ mm and $D = 3$ mm is compared with the results of calculation according to (17) in Fig. 17. However, the Nusselt number in the first and second terms of this equation is calculated taking into account heat transfer in the entrance region of the thermal boundary layer and is determined from the average heat transfer coefficient in accordance with Eq. (16). At that, heat transfer in the entrance region of the thermal boundary layer is calculated by Eq. (14), and heat transfer during condensation is calculated by (10) at $\mathrm{Re} < \mathrm{Re}_*$ or by (5) at $(\mathrm{Re} < \mathrm{Re}_* \le \mathrm{Re}_{cr})$.

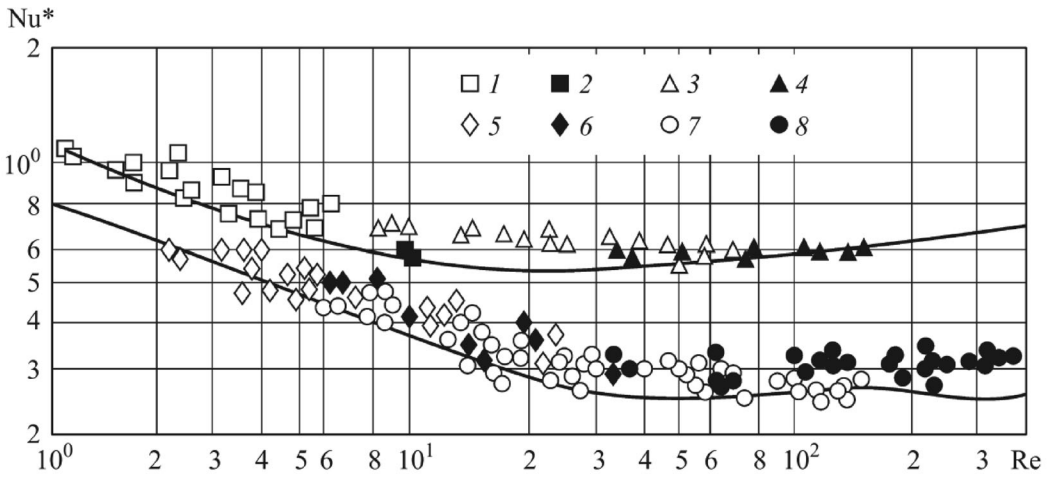

Fig. 17. Comparison of experimental data on heat transfer at R21 condensation on bundles of $D = 16$ mm and $D = 3$ mm tubes with calculation by (17). *1–2*—single cylinder ($D = 3$ mm): *1*—$t_S = 40°$C; *2*—$t_S = 60°$C; *3–4*—bundle: *3*—$t_S = 40°$C; *4*—$t_S = 60°$C. *5–6*: single cylinder ($D = 16$ mm); *5*—$t_S = 40°$C; *6*—$t_S = 60°$C; *7–8*—bundle: *7*—$t_S = 40°$C; *8*—$t_S = 60°$C. Lines—calculation.

As it follows from the data shown earlier in Figs. 4 and 5, during condensation on cylinders which diameter is commensurate with the capillary constant of liquid, there is no laminar film flow. The detached drops of condensate act as wave generators on the film, which propagate along the entire perimeter of the cylinder and lead to heat transfer intensification of up to about 1.5 times in comparison with the calculation according to the Nusselt theory. At $\mathrm{Re} \le 10$, heat transfer on a bundle of tubes with $D = 3$ mm was calculated from the dependence:

$$\mathrm{Nu}^* = \mathrm{Nu}_0^* \varepsilon_\sigma. \tag{18}$$

Empirical coefficient $\varepsilon_\sigma = 1.5$ is taken in accordance with data in Fig. 4.

When calculating heat transfer on a bundle of tubes with $D = 3$ mm, it was taken that the wave regime begins at $\mathrm{Re}_* = 10$ (see Fig. 3). Under these assumptions, the results of calculation by dependence (17) agree satisfactorily with the experimental data. It should be emphasized that heat transfer in the entrance region of the thermal boundary layer in formula (14) depends on the Galileo number (the linear size of the cylinder $(\pi R)^{-1/3}$). That is why there is a significant intensification of heat transfer on the bundle of tubes of a small diameter. In addition, even at $\mathrm{Re} > 50$, the length of the entrance region may exceed the tube half-perimeter, i.e. $L_{ENT} > \pi R$. The condensation process takes place completely in a space between the tubes, and heat transfer in the entrance region of the thermal boundary layer is calculated from dependence (15).

When determining the heat transfer coefficient $K = \frac{1}{\frac{1}{\alpha_{ins}}\frac{D}{d} + \frac{D}{2\lambda}\ln\frac{D}{d} + \frac{1}{\alpha_C}}$ $\left[\frac{\mathrm{W}}{\mathrm{m}^2\cdot\mathrm{K}}\right]$ and calculating q $\left[\frac{\mathrm{W}}{\mathrm{m}^2}\right]$, we can determine the heat transfer area for a device of the desired performance. Here D [m] and d [m] are the outer and inner tube diameters, λ $\left[\frac{\mathrm{W}}{\mathrm{m}\cdot\mathrm{K}}\right]$ is heat conductivity of tube material, α_{ins} $\left[\frac{\mathrm{W}}{\mathrm{m}^2\cdot\mathrm{K}}\right]$ and α_C $\left[\frac{\mathrm{W}}{\mathrm{m}^2\cdot\mathrm{K}}\right]$ are the heat transfer coefficient of water inside the tubes and the heat transfer coefficient during condensation.

The above described algorithm for calculating heat transfer during vapor condensation on a bundle of horizontal tubes of different diameters uses semi-empirical equations based on the fundamental results on hydrodynamics and heat transfer in film flows obtained in numerous studies of different authors.

6. BRIEF ANALYSIS OF THE CURRENT STATE OF THE ART

In publications of recent years, the studies of heat transfer on bundles of smooth tubes continue [16, 61, 62, 71]. Much attention is paid to measuring the local parameters of the film along the

cooled cylinder perimeter during condensation (film thickness, pulsation characteristics of the film, vortex flows inside the film at the points of jet separation from the wall and when liquid contacts the next tube, the tube wall temperature along the perimeter, etc.) [16, 54, 62, 63, 71]. Undoubtedly, such information is new and allows a more accurate understanding of the mechanism of energy transfer during a phase transition. So, in [54] the local heat transfer coefficients along the cylinder perimeter were measured. The high value of the heat transfer coefficient at the frontal point of liquid jet contact with the wall can only be explained by the appearance of a thermal boundary layer.

Another important direction relates to the replacement of freons R11, R12, R22, etc., prohibited by the Montreal Protocol, by other refrigerants. This is an immense field of activity because in addition to experiments on heat transfer during condensation, it is necessary to study the thermophysical properties of new refrigerants or their mixtures, see [16, 54, 56, 58, 60, 64, 65].

It should be borne in mind that heat transfer during boiling and condensation of mixtures, whose composition is far from the azeotrope point, as a rule, decreases several times as compared to heat transfer of a pure component that is part of the mixture. This circumstance leads to an increase in the working surface of heat exchangers. During condensation, one of mixture components can behave as a non-condensable impurity.

The experiments on heat transfer during condensation with new refrigerants are most often carried out on single cylinders [16, 54, 56–58, 60, 64, 66, 68]. It should be noted that the mentioned publications do not contain information on the chromatographic analysis of vapors of substances whose heat transfer is being studied. The authors do not explain the obtained underestimated values of the heat transfer coefficient in comparison with the Nusselt theory. The presence of hundredths of a percent of air or other non-condensable impurities in a vapor, even in small fractions, can significantly reduce the values of experimental data on heat transfer as compared to the calculated ones.

Another important area that attracts the attention of researchers is the methods of enhancing heat transfer during condensation. One of the most common methods of enhancement used in industry is tube finning [16, 54, 56, 68, 69], related to the so-called passive methods of intensification. Active methods of heat transfer enhancement during condensation are also of interest, see, for example review [70]. However, the enhancement of heat transfer during condensation is an extensive topic that goes beyond the scope of this review.

CONCLUSIONS

1. When stationary vapor condenses on single tubes of a small diameter ($\widetilde{D} < 10$), wave formation is observed even at low Re numbers, and the Nusselt number Nu^* is a function of the following criteria: $\mathrm{Nu}^* = f(\mathrm{Re}, \widetilde{D}, \mathrm{Ka})$.

2. In the wave film flow, heat transfer can be considered dependent only on the residual film thickness.

3. During condensation of stationary vapor on a bundle of horizontal tubes, heat transfer is determined by the density of irrigation of a given tube in the bundle.

4. It is shown that the entrance region of the thermal boundary layer is formed on each tube of the bundle, and the total Nusselt number is determined from dependence (15).

5. Satisfactory agreement between the experimental data and the calculation by the semi-empirical algorithm for stationary vapor condensation on a horizontal tube bundle is shown.

NOTATIONS

C_p—specific heat capacity at constant pressure, J/kg·K

D—outer tube diameter, m

d—inner tube diameter, m

g—acceleration of gravity, m^2/s

$L = \pi R$—length of the half-perimeter of the tube, m

L_{ENT}—length of the entrance region, m

$l_\sigma = \sqrt{\sigma/([g\rho_L - \rho_V])}$—capillary constant, m

$l_\nu = \left(\nu^2/g\right)^{1/3}$—viscous-gravitational constant, m

q—heat flux density, W/m^2

Q—heat flux, W

R—tube radius, m

r—latent heat of vaporization, J/kg

Greek Symbols

α—heat transfer coefficient, W/m^{2}K

δ—film thickness, m

λ—heat conductivity, W/(m·K)

μ, ν—dynamic and kinematic viscosity, Pa·s; m^2/s

ρ—density, kg/m^3

σ—surface tension, N/m

τ—shear stress, Pa

Dimensionless Parameters

$\mathrm{Ka} = (l_\sigma/l_\nu)^6 = \sigma^3/\left(\nu^4\rho^3 g\right)$—Kapitza number

$\mathrm{Re} = \frac{U\cdot\delta}{\nu} = \frac{q\cdot L}{\mu r}$—film Reynolds number

Re_*—Reynolds number with $L = l_\sigma$

$\mathrm{Pr} = \mu C_p/\lambda$—Prandtl number

$\mathrm{Ga} = gD^3/\nu^2$—Galileo number

$\mathrm{Nu} = \alpha\cdot L/\lambda$—Nusselt number

$\mathrm{Nu}^* = \alpha\cdot l_\nu/\lambda$—Nusselt number with $L = l_v$

Indices

L—liquid, S—saturation, V—vapor, W—wall, cr—critical, l—laminar, t—turbulent, w—wave.

FUNDING

The work was carried out within the framework of the state assignment to IT SB RAS (project no. 12103100216-1).

CONFLICT OF INTEREST

The authors of this work declare that they have no conflicts of interest.

REFERENCES

1. Joule, J.P., On the Surface-Condensation Steam, *Philos. Trans. Royal Soc. London*, 1861, vol. 151, pp. 133–160.
2. Short, B.E. and Brown, H.E., Condensation of Vapor on Vertical Banks of Horizontal Tubes, *Proc. Inst. Mech. Eng., General Discussion on Heat Transfer, 27*, 1951, vol. 31.
3. Bromley, L.A., Effect of Heat Capacity of Condensate, *Ind. Eng. Chem.*, 1952, vol. 44, no. 12, pp. 2966–2969.
4. Shekriladze, I.G. and Gomelauri, V.I., Theoretical Study of Laminar Film Condensation of Flowing Vapour, *Int. J. Heat Mass Transfer*, 1966, vol. 9, no. 6, 581–591; https://doi.org/10.1016/0017-9310(66)90092-5
5. Fujii, T., Uehara, H., and Kurata, Ch., Laminar Filmwise Condensation of Flowing Vapour on a Horizontal Cylinder, *Int. J. Heat Mass Transfer*, 1972, vol. 15, no. 2, pp. 235–246; https://doi.org/10.1016/0017-9310(72)90071-3
6. Fujii, T., Uehara, H., Hirata, K., and Oda, K., Heat Transfer and Flow Resistance in Condensation of Low Pressure Steam Flowing through Tube Banks, *Int. J. Heat Mass Transfer*, 1972, vol. 15, no. 2, pp. 247–260; https://doi.org/10.1016/0017-9310(72)90072-5
7. Sukhatme, S.P., Jagadish, B.S., and Prabhakaran, P., Film Condensation of R-11 Vapour on Single Horizontal Enhanced Condenser Tubes, *ASME J. Heat Transfer*, 1990, vol. 112, no. 1, pp. 229–234; https://doi.org/10.1115/1.2910350
8. Sreepathi, L.K., Bapat, S.L., and Sukhatme S.P., Heat Transfer during Film Condensation of R-123 Vapour on Horizontal Integral-Fin Tubes, *J. Enhanced Heat Transfer*, 1996, vol. 3, no. 2, pp. 147–164; https://doi.org/10.1615/JEnhHeatTransferv3.i2.70
9. Kumar, R., Varma, H.K., Mohanty, B., and Agrawal, K.N., Augmentation of Outside Tube Heat Transfer Coefficient during Condensation of Steam over Horizontal Copper Tubes, *Int. Comm. Heat Mass Transfer*, 1998, vol. 25, no. 1, pp. 81–91; https://doi.org/10.1016/S0735-1933(97)00139-5
10. McNeil, D.A., Burnside, B.M., and Cuthbertson, G., A Comparison between a Small In-Line and a Staggered Tube Bank Condensing Steam Filmwise at Low Pressures, *Exp. Thermal Fluid Sci.*, 2001, vol. 25, nos. 3/4, pp. 113–123; https://doi.org/10.1016/S0894-1777(01)00085-1
11. Burnside, B.M., Cuthbertson, G., and McNeil, D.A., Pressure Drop Measurements in Condensing Steam over a Horizontal Bundle of Staggered Tubes, *Int. J. Therm. Sci.*, 2001, vol. 40, no. 10, pp. 917–926; https://doi.org/10.1016/S1290-0729(01)01278-9
12. Eckels, S.J., Effects of Inundation and Miscible Oil upon Condensation Heat Transfer Performance of R-134a, *ASHRAE Rep.*, 2002, vol. 984.
13. Browne, M.W. and Bansal, P.K., An Overview of Condensation Heat Transfer on Horizontal Tube Bundles, *Appl. Thermal Eng.*, 1999, vol. 19, no. 6, pp. 565–594; https://doi.org/10.1016/S1359-4311(98)00055-6
14. Cavallini, A., Censi, G., Del Col, D., Doretti, L., Longo, G.A., Rossetto, L., and Zilio, C., Condensation inside and outside Smooth and Enhanced Tubes—A Review of Recent Research, *Int. J. Refr.*, 2003, vol. 26, no. 4, pp. 373–392; https://doi.org/10.1016/S0140-7007(02)00150-0
15. Miyara, A., Condensation of Hydrocarbons—A Review, *Int. J. Refr.*, 2008, vol. 31, no. 4, pp. 621–632; https://doi.org/10.1016/j.ijrefrig.2007.12.003
16. Bonneau, C., Josset, C., Melot, V., and Auvity, B., Comprehensive Review of Pure Vapour Condensation outside of Horizontal Smooth Tubes, *Nuclear Eng. Design*, 2019, vol. 349, pp. 92–108; https://doi.org/10.1016/j.nucengdes.2019.04.005
17. Cuthbertson, G., An Experimental Investigation of Dropwise and Filmwise Condensation of Low Pressure Steam in Tube Banks, Doctoral dissertation, Heriot-Watt University, 1999, vols. 1/2.
18. Gstöhl, D., Heat Transfer and Flow Visualization of Falling Film Condensation on Tube Arrays with Plain and Enhanced Surfaces, Thesis. EPFL, 2004.
19. Butterworth, D., Inundation without Vapour Shear, in *Power Condenser Heat Transfer Technology: Computer Modeling, Design, Fouling*, Hemisphere Publ., 1981. pp. 271–277.
20. Butterworth, D., Application of the Models to Bundles of Horizontal Tubes, in *Heat Exchanger Design Handbook*, Hemisphere Publ., 1983, vol. 2, pp. 10–12.
21. Kedzierski, M., Chato, J., and Rabas, T., Condensation, in *Handbook of Heat Transfer*, Wiley, 2003.
22. Bejan, A., Fundamental Principles, in *Convection Heat Transfer*, 3d ed., Wiley, 2004, pp. 1–29.
23. Isachenko, V.P., *Teploobmen pri kondensatsii* (Heat Transfer in Condensation), Moscow: Energiya, 1977.
24. Krektunov, O.P. and Savus, A.S., *Processy‘ kondensatsii i kondensatory maslozhirovogo proizvodstva* (Processes of Condensation and Condensers of Oil and Fat Production), Firsova E.P., Ed., St. Petersburg, 1998.
25. Milman, O.O. and Fedirov, V.A. *Kondensatory paroturbinnykh ustanovok* (Air Condensing Units), Moscow: MEI, 2002.
26. Gogonin, I.I., *Issledovanie teploobmena pri plenochnoi kondensatsii para* (Investigation of Heat Transfer during Film Condensation of Vapor), Novosibirsk: SB RAS, 2015.

27. *Standards for Steam Surface Condensers*, 11th ed., Cleveland: Heat Exchange Institute, 2012.
28. Nusselt, W., Die Oberfluchenkondensation des Wasserdampfes, *VDI-Zc*, vol. 60, 1916.
29. Brauer, H., Stromung and Warmeubergang bei Rieselfilmen, *VDI Forschungself*, vol. 457 (1956), B22.
30. Kholostykh, V.I., Blyakher, I.G., and Shekhtman, A.A., Flow of a Liquid Film along a Vertical Surface, *J. Eng. Phys. Thermophys.*, 1972, vol. 22, no. 3, pp. 348–351; https://doi.org/10.1007/BF00829469
31. Alekseenko, S.V., Nakoryakov, V.E., and Pokusaev, B.G., *Wave Flow of Liquid Films*, New York: Begell House, 1994.
32. Kutateladze, S.S. and Nakoryakov, V.E., *Teplomassoobmen i volny v gazozhidkostnykh sistemakh* (Heat and Mass Transfer and Waves in Gas-Liquid Systems), Novosibirsk: Nauka, 1984.
33. Colburn, A.P., Calculation of Condensation with a Portion of Condensate Layer in Turbulent Motion, *Ind. Eng. Chem.*, 1934, vol. 26, no. 4, pp. 432–434; https://doi.org/10.1021/ie50292a016
34. Berman, L.D., et al., Heat Transfer during Film Condensation of Steam on Transversely Streamlined Horizontal Pipes, in *Konvektivnaya teploperedacha v dvukhfaznom i odnofaznom potokakh* (Convective Heat Transfer in Two-Phase and Single-Phase Flows), Borishansky, V.M. and Paleyev, I.I., Eds., Moscow: Energia, 1964, pp. 7–53.
35. Gogonin, I.I. and Kataev, A.I., Methodological Errors in Experimental Studies of Heat Transfer during Condensation, *Thermal Eng.*, 2000, vol. 12, pp. 48–53.
36. Gogonin, I.I., Sosunov, V.I., and Kataev, A.I., Heat Transfer during Condensation of Water Steam on a Bundle of Horizontal Pipes, *Thermal Eng.*, 1992, vol. 4, pp. 48–51.
37. Milman, O.O. and Shklover, G.G., Dependence of the Averaged Values of Heat Transfer and Heat Transfer Coefficients on the Method of Averaging, *Thermal Eng.*, 1977, vol. 4, pp. 24–29.
38. Shklover, G.G., Usachev, A.M., and Kopp, M.I., Heat Transfer and Hydrodynamics during Condensation of Steam on a Horizontal Pipe, in *Two-Phase Flows: Heat Transfer and Hydrodynamics, Materials of the 7th All-Union Conf., October, 1985.*
39. Berman, A.D. and Fuks, S.N., Influence of Air Admixture on Heat Transfer during the Condensation of Moving Steam, *News All-Union Thermal Engin. Inst.*, 1952, vol. 11, pp. 11–48.
40. Isachenko, V.P. and Glushkov, A.F., Heat Transfer during Steam Condensation on a Horizontal Pipe and Condensate Flow From Above, *Thermal Eng.*, 1969, vol. 6, p. 79.
41. Wanniarachchi, A.S., Marto, P.J., and Rose, J.W., Film Condensation of Steam on Horizontal Finned Tubes: Effect of Fin Spacing, *J. Heat Transfer*, 1986, vol. 108, no. 4, pp. 960–966.
42. Young, E.H. and Briggs, D.E., The Condensing of Low Pressure Steam on Vertical Rows of Horizontal Copper and Titanium Tubes, *AIChE J.*, 1966, vol. 12, no. 1, pp. 31–35; https://doi.org/10.1002/aic.690120109
43. Mills, A.F., Tan, C., and Chung, D.K., Experimental Study of Condensation from Steam-Air Mixtures Flowing over a Horizontal Tube: Overall Condensation Rates, in *Int. Heat Transfer Conf. Digital Library*, Begel House, 1977.
44. Ferguson, R.M. and Oakden, J.C., Heat Transfer Coefficients for Water and Steam in a Surface Condenser, in *Transaction of Chem. Eng. Congress (World Power Conf.)*, 1936, vol. 4, pp. 1–32.
45. Gogonin, I.I., Hydrodynamics and Heat Transfer during Condensation of Stationary Steam on a Horizontal Cylinder, *Izv. SO AN USSR. Ser. Tech. Nauk*, 1986, vol. 10, no. 2, pp. 24–32.
46. Gogonin, I.I., Dorokhov, A.R, and Sosunov, V.I., Heat Transfer during Condensation of Stationary Steam on a Bundle of Smooth Horizontal Tubes, *Thermal Eng.*, 1977, vol. 4, pp. 23–36.
47. Kutateladze, S.S. and Gogonin, I.I., Heat Transfer in Film Condensation of Slowly Moving Vapour, *Int. J. Heat Mass Transfer*, 1979, vol. 22, no. 12, pp. 1593–1599; https://doi.org/10.1016/0017-9310(79)90075-9
48. Kutateladze, S.S., Gogonin, I.I., and Sosunov, V.I., Experimental Study of Heat Transfer during Condensation of Stationary Vapor on a Bundle of Smooth Horizontal Tubes, *Theor. Found. Chem. Eng.*, 1979, vol. 13, pp. 716–720.
49. White, R.E., Condensation of Refrigerant Vapors—Apparatus and Film Coefficients for Freon-12, *Trans. Am. Soc. Mech. Engin.*, 1948, vol. 70, no. 6, pp. 689–693; https://doi.org/10.1115/1.4017818
50. Chernobylsky, I.I. and Gorodinskaya, S.A., Investigation of Heat Transfer during Condensation of Ammonia Vapors on the Outer Surface of Pipes, *Procs. Inst. Thermal Power Engin. Acad. Sci. Ukr. SSR, Kyiv*, 1961, vol. 4, pp. 44–54.
51. Gogonin, I.I., Sosunov, V.I., Lazarev, S.I., and Kabov, O.A., Heat Transfer while Stationary Vapor Condensation on a bundle of Horizontal Tubes with Different Configuration, *Teploenergetika*, 1982, vol. 3, pp. 33–36.
52. Rogers, J.T., Laminar Falling Film Flow and Heat Transfer Characteristics on Horizontal Tubes, *Canad. J. Chem. Eng.*, 1981, vol. 59, no. 2, pp. 213–222; https://doi.org/10.1002/cjce.5450590212
53. Kutateladze, S.S., Gogonin, I.I., and Sosunov, V.I., The Influence of Condensate Flow Rate on Heat Transfer in Film Condensation of Stationary Vapour on Horizontal Tube Banks, *Int. J. Heat Mass Transfer*, 1985, vol. 28, no. 5, pp. 1011–1018; https://doi.org/10.1016/0017-9310(85)90283-2

54. Park, K.J. and Jung, D., Condensation Heat Transfer Coefficients of Flammable Refrigerants on Various Enhanced Tubes, *J. Mech. Sci. Technol.*, 2005, vol. 19, no. 10, pp. 1957–1963; https://doi.org/10.1007/BF02984275
55. Parken, W.H., Fletcher, L.S., Sernas, V., and Han, J.C., Heat Transfer through Falling Film Evaporation and Boiling on Horizontal Tubes, *ASME J. Heat Transfer*, 1990, vol. 112, no. 3, pp. 744–750; https://doi.org/10.1115/1.2910449
56. Sajjan, S.K., Kumar, R., and Gupta, A., Experimental Investigation during Condensation of R-600a Vapor over Single Horizontal Integral-Fin Tubes, *Int. J. Heat Mass Transfer*, 2015, vol. 88, pp. 247–255; https://doi.org/10.1016/j.ijheatmasstransfer.2015.04.079
57. Sajjan, S.K., Kumar, R., and Gupta, A., Experimental Investigation of Vapor Condensation of Iso-Butane over Single Horizontal Plain Tube under Different Vapor Pressures, *Appl. Thermal Eng.*, 2015, vol. 76, pp. 435–440; https://doi.org/10.1016/j.applthermaleng.2014.11.049
58. Ji, W.T., Chong, G.H., Zhao, C.Y., Zhang, H., and Tao, W.Q., Condensation Heat Transfer of R134a, R1234ze(E), and R290 on Horizontal Plain and Enhanced Titanium Tubes, *Int. J. Refr.*, 2018, vol. 93, pp. 259–268; https://doi.org/10.1016/j.ijrefrig.2018.06.013
59. Li, W., Sun, Z.C., Guo, R.H., Ma, X., Liu, Z.C., Kukulka, D.J., Ayub, Z., Chen, W., and He, Y., Condensation Heat Transfer of R410A on Outside of Horizontal Smooth and Three-Dimensional Enhanced Tubes, *Int. J. Refr.*, 2019, vol. 98, pp. 1–14; https://doi.org/10.1016/j.ijrefrig.2018.09.035
60. Gebauer, T., Al-Badri, A.R., Gotterbarm, A., El Hajal, J., Leipertz, A., and Fröba, A.P., Condensation Heat Transfer on Single Horizontal Smooth and Finned Tubes and Tube Bundles for R134a and Propane, *Int. J. Heat Mass Transfer*, 2013, vol. 56, nos. 1/2, pp. 516–524; https://doi.org/10.1016/j.ijheatmasstransfer.2012.09.049
61. Grzebielec, A. and Rusowicz, A., Thermal Resistance of Steam Condensation in Horizontal Tube Bundles, *J. Power Technol.*, 2011, vol. 91, no. 1, p. 41.
62. Li, S. and Ju, Y., Numerical Study on the Condensation Characteristics of Various Refrigerants outside a Horizontal Plain Tube at Low Temperatures, *Int. J. Thermal Sci.*, 2022, vol. 176, p. 107508; https://doi.org/10.1016/j.ijthermalsci.2022.107508
63. Zhao, C.Y., Ji, W.T., Jin, P.H., Zhong, Y.J., and Tao, W.Q., Hydrodynamic Behaviors of the Falling Film Flow on a Horizontal Tube and Construction of New Film Thickness Correlation, *Int. J. Heat Mass Transfer*, 2018, vol. 119, pp. 564–576; https://doi.org/10.1016/j.ijheatmasstransfer.2017.11.086
64. Kumar, R., Varma, H.K., Mohanty, B., and Agrawal, K.N., Condensation of R-134a Vapor over Single Horizontal Circular Integral-Fin Tubes, *Heat Transfer Eng.*, 2000, vol. 21, no. 2, pp. 29–39; https://doi.org/10.1080/014576300271004
65. Cavallini, A., Censi, G., Del Col, D., Doretti, L., Longo, G.A., and Rossetto, L., Experimental Investigation on Condensation Heat Transfer and Pressure Drop of New HFC Refrigerants (R134a, R125, R32, R410A, R236ea) in a Horizontal Tube, *Int. J. Refr.*, 2001, vol. 24, no. 1, pp. 73–87; https://doi.org/10.1016/S0140-7007(00)00070-0
66. Jung, D., Kim, C.B., Cho, S., and Song, K., Condensation Heat Transfer Coefficients of Enhanced Tubes with Alternative Refrigerants for CFC11 and CFC12, *Int. J. Refr.*, 1999, vol. 22, no. 7, pp. 548–557; https://doi.org/10.1016/S0140-7007(99)00020-1
67. Kutateladze, S.S. , Gogonin, I.I., Dorokhov, A.R., and Sosunov, V.I., Heat Transfer in Vapor Condensation on a Horizontal Tube Bundle, *Heat Transfer Sov. Res.*, 1981, vol. 13, no. 3, pp. 32–50.
68. Kumar, R., Varma, H.K., Mohanty, B., and Agrawal, K.N., Prediction of Heat Transfer Coefficient during Condensation of Water and R-134a on Single Horizontal Integral-Fin Tubes, *Int. J. Refr.*, 2002, vol. 25, no. 1, pp. 111–126; https://doi.org/10.1016/S0140-7007(00)00094-3
69. Briggs, A. and Rose, J.W., Effect of Fin Efficiency on a Model for Condensation Heat Transfer on a Horizontal, Integral-Fin Tube, *Int. J. Heat Mass Transfer*, 1994, vol. 37, no. 1, pp. 457–463; https://doi.org/10.1016/0017-9310(94)90045-0
70. Hughes, M.T. and Garimella, S., A Review of Active Enhancement Methods for Boiling and Condensation, *Int. J. Heat Mass Transfer*, 2024, vol. 218, p. 124752; https://doi.org/10.1016/j.ijheatmasstransfer.2023.124752.
71. Belghazi, M., Bontemps, A., Signe, J.C., and Marvillet, C., Condensation Heat Transfer of a Pure Fluid and Binary Mixture Outside a Bundle of Smooth Horizontal Tubes. Comparison of Experimental Results and a Classical Model, *Int. J. Refr.*, 2001, vol. 24, no. 8, pp. 841–855; https://doi.org/10.1016/S0140-7007(00)00037-2